LBL--26321

DE90 001424

RECENT ADVANCES IN DETECTORS FOR SINGLE-PHOTON COUNTING

Branko Leskovar
Lawrence Berkeley Laboratory
Engineering Division
One Cyclotron Road
Berkeley, California 94720 U.S.A.

The time-correlated single-photon counting method has gained wide acceptance for investigating time behaviors of the fluorescence associated with electronic energy relaxation of excited molecules, optical ranging and communication experiments, plasma diagnostics and optical time domain reflectometry. The measurement of fluorescence lifetimes in studying the photophysical properties of organic molecules require photon detectors with high sensitivity and fast time response. The time width of the measuring system response in time-correlated single-photon counting experiments using picosecond light excitation is mainly determined by the single photoelectron time spread of photon detector. Recent progress that has been made in fast high-gain detectors using photoemission and secondary emission processes is reviewed and summarized. Specifically, performance characteristics are presented and compared of the ITT F4129, Hamamatsu R1564U and R2287U extended lifetime microchannel plate photomultipliers. Also characteristics of the Amperex XP2020 and RCA C31024 conventionally design photomultipliers are presented. Finally, the silicon avalanche photodiodes are compared with respect to their preliminary performance in time-correlated single-photon counting applications.

Introduction

The time-correlated single-photon counting method has gained wide acceptance for investigating fluorescence time behaviors associated with electronic energy relaxation of excited molecules, optical ranging and communication experiments, plasma diagnostics and optical time domain reflectometry. Fluorescence lifetime measurements for studying the

---

photophysical properties of organic molecules place a special requirement of sensitivity and fast time response on photon detectors.[1,2] During the past sixteen years the method has proved to be extremely powerful and has added significantly to our understanding of the dynamic physical and chemical processes which are important in molecular biology. Particularly important are measurements of the changes in fluorescence parameters which occur with changes in temperature, pH factor, ionic strength, salt composition and other factors when molecules are in solutions.

Among the different techniques available for subnanosecond fluorescence lifetime measurements,[1-5] the time-correlated single-photon counting method has gained wide acceptance. The sample is repeatedly excited with short light pulses and the resulting fluorescent pulses adjusted in intensity so that for most of the light flashes only one photoelectron is produced at the photocathode of a fast high-gain photon detector. This counting technique of lifetime measurement is based upon the concept that the probability distribution for the emission of a single photon of fluorescence following a single exciting light pulse is identical to the intensity-time profile of the cascade of all the photons which are emitted following a single flash of exciting light. The single photon emission probability distribution is built up by repetitive exposure of the sample to short bursts of exciting light and recording of the time of arrival of the first photon of fluorescence following each exciting pulse. This is the most sensitive of techniques for measuring lifetimes, offering excellent signal-to-noise ratio, wide dynamic range of several decades of light intensity, and subnanosecond lifetime measurement capabilities.[5] Measurements have shown that in situations where a subnanosecond lifetime must be accurately measured, the fundamental limitations on the precision of measurements are due to the following factors: the fluctuations in the light pulse waveshape, the single-photoelectron time spread of the photon detector,[6-7] the dependence of the measuring system on the excitation and emission

wavelengths and the timing error introduced by the discriminator or other circuit elements used in the system. Consequently, a high-precision measuring system should operate with the shortest possible exciting light pulses, because the time spread in the light pulse waveshape is in absolute amounts smaller for narrower pulses. Also, the fastest photon detector with adequate gain and small afterpulsing phenomenon operated under an optimized condition[8-10] must be used, since it will have a relatively smaller value of single-photoelectron time spread.

Single Photoelectron Time Spread Considerations

In a typical electrostatically focused photomultiplier the single photoelectron transit time spread is mainly caused by fluctuations of individual times of flight of photoelectrons and secondary electrons due to their different trajectories and their initial velocity differences, Fig. 1. The factors that contribute to the transit time spread are differences in trajectory length and in electrical field strength for different portions of the photocathode-first-dynode region, and between various dynode sections.

The total single photoelectron transit time spread consists of the photoelectron transit time spread between the photocathode and the first dynode of the multiplier, the electron transit time spread in the electron multiplier, and that between the electron multiplier and the anode.[6-9] The major causes of transit time spreads are the distribution of initial emission velocities of photoelectrons and secondary electrons, unequal electron path lengths between different electrodes and nonuniform electric fields. Generally, the initial stages of a photomultiplier contribute the greatest weight to the total transit time spread. In the latter stages, the larger number of electrons in the pulse provide many samples of transit time through the stage and reduce the transit time spread of that stage in the manner of the standard error of mean value. The variance of the total single photoelectron transit time, t^2, is approximately given by the following equation[6]:

$$t^2 \approx t_{CD1}^2 + \frac{t_{D1D2}^2}{g_1}(1+g^2{}_1) + \frac{t_{DD}^2}{g_1(g-1)}(1+g^2) \tag{1}$$

where t_{CD1}^2 is the variance of the photoelectron transit time between the photocathode and the first dynode, t_{D1D2}^2 is the variance of the electron transit time between the first and the second dynode, t_{DD}^2 is the variance of the electron transit time between two successive dynodes, g_1 is the gain of the first dynode, g is the gain of all other dynodes, $g^2{}_1$ is the variance of the gain g_1, and g^2 is the variance of the gain g.

A total single photoelectron transit time spread, expressed by the full width of half maximum, is related to the standard deviation of the total transit time by the expression:

$$t_{FWHM} \approx 2.36t \tag{2}$$

The contribution to the transit time spread by the unequal electron path lengths between different electrodes and the nonuniformity of electric fields at the dynodes can be minimized by proper design of the input electron optics and the electron multiplier. Therefore, this contribution can be made small enough so that the ultimate limitation on time spread is determined by initial velocity effects of photoelectrons and secondary electrons. Assuming a uniform electric field between the photocathode and the first dynode, and equal photocathode-to-first-dynode electron path lengths, the time spread between a photoelectron emitted with zero initial velocity and a photoelectron with velocity v_o is approximately given by the following equation[6]:

$$\Delta t_n \approx \frac{v_o l}{eV} m_o \tag{3}$$

where l is the distance between the photocathode and the first dynode, V is the voltage between the photocathode and the first dynode, and e and m_0 are the charge and mass of an electron, respectively.

It can be seen from this equation that transit time spread resulting from the initial velocity distribution is decreased by increasing the voltage between the photocathode and the first dynode. Similar considerations are valid for the secondary electron initial velocities in an electron multiplier.

It was shown in earlier papers that photomultipliers using a microchannel plate electron multiplier exhibit significantly better time resolution capabilities than conventionally designed electrostatically focused photomultipliers.[11-17]

The microchannel plate consists of a two dimensional array of thousand (or millions) of very small diameter short channel electron multipliers closely packed parallel to each other. Figure 2 shows the configuration of a typical plate.

Each electron multiplying channel is a continuous glass tube whose inside surface has a high resistance semiconductor coating which serves as a secondary electron-emitting surface. The array of glass microchannels are connected electrically in parallel by metal electrodes on opposite faces of the plate which is operated in high vacuum with a voltage applied between the two faces. When a voltage of about 1000V is applied between the electrodes, the semiconducting coating inside each microchannel provides a continuous potential gradient along its length. Incident photoelectron at the input end of the microchannel ejects electrons which are accelerated down the channel toward the positive end; the electrons collide with the wall of the channel many times while passing down the channel. The voltage gradient and channel diameter are adjusted so that, on the average, substantially more than one secondary electron is released at each collision. This is illustrated in Fig. 3.

Microchannels typically have diameters ranging from 6 to 50 μm and are spaced by distances ranging from 8 to 60 μm. The channel lengths are between 0.5 to 2.0 mm. Typically, a potential difference of 1000V across the microchannel plate will produce gains

of about 10^3 to 10^4 for straight microchannels with the channel length-to-diameter ratio of 40. Because of the small channel size and high voltage involved, the total electron transit time is significantly shorter than for a conventional electron multiplier structure having the same gain.

Typical electron gain voltage characteristics of single microchannel plates with straight and curved channels, and for channel chevron plates are shown in Fig. 4. The characteristics are given for an input signal current density of $10^{-12}A/cm^2$ and with an input electron energy of 300 eV for both the straight channel plate and the chevron plate. Both types of plates have a total standing current along the walls of channels (total of all channels) of 0.8 μA.

The electron gain of the microchannel plate is determined by the applied voltage and the length-to-diameter, L/d, of microchannels used in a particular plate. Above a certain value of the plate gain, the ion feedback leads to repetitive electron avalanches which saturate the channel, and cause field distortion due to wall charging. Both effects lead to temporary loss of gain at the plate output. As expected, the curved channel plate can be operated at a much higher gain before ion feedback causes gain saturation effects.

Based on the above mentioned work, further effort has been made to investigate and review the time and pulse-height resolution of some new generation commercially available photomultipliers. The measurements of the characteristics of these photomultipliers were made with a measuring system which has previously been described in Reference 6. The system has a time resolution of approximately 25 ps, FWHM.

Specifically, performance characteristics have been studied of the new Amperex XP2020 and RCA C31024 photomultipliers which use conventional multiplier structures. Furthermore, the characteristics have been investigated of a new generation of ITT F4129, Hamamatsu R1564U and R2287U extended life microchannel plate photomultipliers. Finally, silicon avalanche photodiodes are compared with respect to their preliminary

performance in time-correlated single-photon counting applications.

The electrostatically focused Amperex XP2020 photomultiplier uses a 12 stage discrete dynode structure with a semi-transparent bialkali SbKCs photocathode having a useful diameter of 45 mm. Its peak spectral response is at 400 nm with a quantum efficiency of 26%. The photomultiplier has copper berillium dynodes instead of AgMgOS dynodes which were used previously in a similar device. The tube design is optimized to have a small single electron time spread and for high repetition rates in counting operations.

The RCA (Burle Tube Products) C31024 photomultiplier has a bialkali photocathode and five high gain gallium-phosphide dynodes. The photocathode has a peak response at 400 nm and a quantum efficiency of 27%. The minimum useful photocathode diameter is 46 mm.

The ITT F4129 photomultiplier has an S-20 photocathode with a maximum usable diameter of 18 mm and three microchannel plates in cascade for the electron multiplication. The plates are in a Z-configuration to reduce the positive ion feedback. The three plates are identical, having 12 μm diameter channels with length to diameter ratios of 40. Proximity focusing is used for the input and collector stages. In ITT F4129f device a protective film is provided between the photocathode and the microchannel plate which leads to a significant improvement in quantum efficiency, stability and life expectancy as well as in the total elimination of the afterpulses.

The Hamamatsu R1564U photomultiplier has a bialkali photocathode with a usable diameter of 18 mm, and two microchannel plates in cascade for electron multiplication.[17] The anode is matched to a 50 Ohm connector. The entrance of the first microchannel plate is covered with a thin aluminum film to prevent the bombardment of the photocathode by positive ions. As in the ITT photomultiplier this results in a significant increase in photocathode life, and stability of quantum efficiency.

The Hamamatsu R2287U photomultiplier like the R1564U has a bialkali photocathode with a maximum usable diameter of 18 mm but has three microchannel plates in cascade for the electron multiplication.[17] The anode is matched to a 50 Ohm connector. Again the entrance face of the first microchannel plate is covered by a thin aluminum film to prevent bombardment of the photocathode by positive ions.

The life of a microchannel plate photomultiplier without protective film is determined by a decrease in the photocathode quantum efficiency because of photocathode positive ion bombardment. The second determining factor is change in the channel wall secondary emission coefficient due to electron scrubbing, especially in high gain region of a channel. This is not effected by the protective film. The life of a device is defined as a total charge density accumulated at the anode at which device losses 50% of its overall responsivity.

Results and Discussions

The results of the measurements of characteristics of the Amperex XP2020, RCA C31024, ITT F4129, Hamamatsu R1564U and R2287U photomultipliers are summarized in Table 1. Also, some of the results are presented in Figs. 5-6.

With full photocathode illumination, and with a light pulse produced by a 200 ps electrical pulse, the rise time, impulse response (FWHM), and single photoelectron time spread (FWHM), were 1.5 ns, 2.4 ns, and 0.51 ns, respectively for the XP2020. Measurement of the dark pulse spectrum showed that the photomultiplier pulse-height resolution is not good enough to show the one, two and three photoelectron peaks. This is typical for all conventionally designed photomultipliers using the first dynode with low gain.

The rise time, impulse response, and single photoelectron time spread for the C31024 photomultiplier were 0.8 ns, 1.0 ns and 0.4 ns, respectively. This device utilizes a negative-electron-affinity GaP (Cs) secondary emission surface on all five dynodes of the electron multiplier resulting in very fast time response and a high pulse-height spectrum

resolution. With the spectrum peak-to-valley ratio of 2.17:1 an effective separation of spurious single photoelectron peak and the desired multiphotoelectron peaks can be achieved. The C31024 has shown resolution of four distinct photoelectron peaks.

The F4129 microchannel plate photomultiplier has a rise time, impulse response and single photoelectron time spread of 0.35 ns, 0.52 ns, and 0.2 ns, respectively. The device exhibits excellent timing capabilities and is significantly less sensitive to ambient magnetic fields than the best conventionally designed photomultipliers. This is mostly due to the small thickness of microchannel plates (approximately 2 mm), very strong applied electric field (5-10 kV/cm) and proximity focusing used between the photocathode and microchannel plate. Figure 5 shows two single photoelectron spectra spaced 1 ns apart. Figure 6 shows the photomultiplier pulse-height spectrum indicating the peak to valley ratio of 2.47:1 with optimized operating conditions. The F4129 has resolved four distinct photoelectron peaks. Also, the life of new generation F4129f device with a 7 nm thick ion barrier film is significantly increased when compared with the life of F4129.

The risetime, impulse response, and single photoelectron time spread for R2287U microchannel plate photomultiplier were approximately 0.28 ns, 0.62 ns and 0.10 ns, respectively.

Afterpulse time spectra measurements made on an ITT F4129f and a Hamamatsu R15764U have shown that the introduction of the protective film has resulted in total elimination of afterpulses. In contrast, all microchannel plate photomultipliers without protective film made by various manufacturers have demonstrated a strong afterpulsing phenomena and a photocathode quantum efficiency decrease during operating time.

In addition to above mentioned photomultipliers, silicon avalanche photodiodes have been recently considered for time-correlated single-photon counting applications.[18-21] Although they are not expected to attain such high resolution as photomultipliers, they have

been considered as a possible alternative to conventionally designed and microchannel plate photomultipliers where ruggedness, small dimensions, low cost and low operating voltage are important. Also, avalanche photodiode can provide significantly higher quantum efficiency in the near infrared wavelength range. Suitable devices are commercially available with photosensitive active diameter of approximately 0.5 mm. This is sufficient for some applications although it is considerably smaller than that of typical photomultipliers.

For photon counting applications the avalanche diode is usually operated in the so called Geiger mode and is reverse biased beyond breakdown. An active quenching method is used to recognize the presence of photodetection as soon as possible after the event and an associate electronic circuit is employed to rapidly switch off the avalanche process and reset the diode allowing the next photodetection to occur. Preliminary measurements performed on RCA C30921S diode have shown that the best time resolution of 400 ps, FWHM, can be obtained with the device cooled at -40^{o}C and operating it with the maximum excess bias voltage of 40 V. Measurements were made using pulse laser diode as a light source, generating pulses of 40 ps in duration at 785 nm wavelength. Cooling device to -40^{o}C was necessary to reduce the dark pulse count rate. The dark pulse count rate was approximately 20×10^3 counts per second at -40^{o}C with the device biased 40 V above the breakdown voltage. At 0^{o}C ambient temperature the dark pulse count rate was 240×10^3 counts per second at the same biasing voltage. This device can be operated at room temperature only if a fast gating of its output is used.

Table 1. Summary Characteristics Measurements of New Generation Conventionally Designed and Microchannel Plate Photomultipliers. Full Photocathode Illumination.

	Amperex XP2020	RCA C31024	ITT F4129	Hamamatsu R1564U	Hamamatsu R2287U
DC Gain	$>3\times10^7$	$>10^6$	1.6×10^6	5×10^5	5×10^6
Supply Voltage Between Anode and Cathode (V)	2200	4000		3400	3600
Microchannel Plate Voltage (V)			2500		
Rise Time (ns)	1.5	0.8	0.35[a]	0.27	0.28
Electron Transit Time (ns)	28	16.2	2.5[a]	0.58	0.62
Impulse Response, FWHM,(ns)	2.4	1.0	0.52[a]		
Single Photoelectron Time Spread, FWHM, (ns)	0.51	0.4	<0.20[a]	0.09	0.10
Multiphotoelectron Time Spread, FWHM, (ns)	0.12[b]	0.058[e]	0.10[d]		
Peak-to-Valley Ratio of Pulse-Height Spectrum with Optimized Operating Conditions		2.17:1	2.47:1[f]		
Dark Pulse Count[g] (cps)	450		1800		
Quantum Efficiency %	26	27	20	15	15
Photocathode Diameter (mm)	44	46	18	18	18

[a] These characteristics were measured for prototype packaged photomultipliers.

[b] Measured using 2500 photoelectrons per pulse.

[c] Measured using 100 photoelectrons per pulse.

[d] Measured using 800 photoelectrons per pulse.

[e] Measured using 1000 photoelectrons per pulse.

[f] Optimized operating condition for F4129 was V_M = 2710V. In this case the photomultiplier gain was 6.6×10^7.

[g] Dark pulse summation is defined by: $\sum_{1/8\ \text{photoelectrons}}^{16\ \text{Photoelectrons}}$ = counts per second.

Acknowledgment

This work was performed as part of the program of the Electronics Research and Development Group, Electronics Engineering Department of the Lawrence Berkeley Laboratory, University of California, Berkeley. The work was partially supported by the U.S. Department of Energy under Contract Number DE-AC03-76SF00098. Reference to a company or product name does not imply approval or recommendation of the product by the University of California or the U.S. Department of Energy to the exclusion of others that may be suitable.

References

1. Time-Resolved Fluorescence Spectroscopy in Biochemistry and Biology, R.B. Cundall and R.E. Dale, Eds., Plenum Press, New York (1983).

2. D.V. O'Connor and D. Phillips, Time-Correlated Single- Photon Counting, Academic Press, New York (1984).

3. P.R. Hartig, K.H. Sauer, C.C. Lo and B. Leskovar, Measurement of Very Short Fluorescence Lifetimes by Single Photon Counting, Rev. Sci. Instr., 47, No. 9, 1122-1129 (1976).

4. B. Leskovar, C.C. Lo, P.R. Hartig and K.H. Sauer, Photon Counting System for Subnanosecond Fluorescence Lifetime Measurements, Rev. Sci. Instr., 47, No. 9, 1113-1121 (1976).

5. B. Leskovar, Nanosecond Fluorescence Spectroscopy, IEEE Trans. Nucl. Sci., NS-32, No. 3, 1232-1241 (1985).

6. B. Leskovar and C.C. Lo, Single Photoelectron Time Spread Measurement of Fast Photomultipliers, Nucl. Inst. Meth., 123, No. 1, 145-160 (1975).

7. B. Leskovar, Accuracy of Single Photoelectron Time Spread Measurement of Fast Photomultipliers, Nucl. Inst. Meth., 128, 115-119 (1975).

8. B. Leskovar, Time Resolution Performance Studies of High-Speed Photon Detectors, Proc. of the 4th International Congress, Laser 79-Optoelectronics, Munich, West Germany, 581-586. Pub. by IPC Science and Technology Press Ltd., England (1979).

9. B. Leskovar, Recent Advances in High-Speed Photon Detectors, Proc. of the 6th International Congress, Laser 83-Optoelectronics, Munich, West Germany. Pub. by Springer Verlag: Optoelectronics in Engineering, 68-74 (1984).

10. B. Leskovar, The Afterpulse Time Spectra of High-Speed Photon Detectors, Proceedings of the 7th International Congress, Laser 85-Optoelectronics, Munich, West Germany. Published by Springer Verlag: Optoelectronics in Engineering, 148-157 (1986).

11. B. Leskovar, Microchannel Plates, Physics Today, 30, No. 11, 42-45 (1977).

12. B. Leskovar and C.C. Lo, Studies of Prototype High-Gain Microchannel Plate Photomultipliers, IEEE Trans. Nucl. Sci. NS-26, No. 1, 388-394 (1979).

13. D.H. Ceckowski, E. Eberhard and E. Carney, Proximity Focused Microchannel Plate Photomultiplier Tubes, IEEE Trans. Nucl. Sci. NS-28, 677-682 (1981).

14. C.C. Lo and B. Leskovar, Performance Studies of High-Gain Photomultiplier Having Z-Configuration of Microchannel Plates, IEEE Trans. Nucl. Sci., NS-28, No. 1, 698-704 (1981).

15. B. Leskovar and T.T. Shimizu, Time Resolution Performance Studies of Hamamatsu R1564U Microchannel Photomultiplier, IEEE Trans. Nucl. Sci., NS-34, No. 1, 427-430 (1987).

16. I. Yamazaki, N. Tamai, H. Kume, T. Tsuchiya and K. Oba, Microchannel-Plate Photomultiplier Applicability to the Time-Correlated Photon-Counting Method, Rev. Sci. Instrum, 56, No. 6, 1187-1193 (1985).

17. Microchannel Plate Photomultiplier Tubes (MCP-PMTS), Hamamatsu Technical Data Sheet, No. T-112 (February 1987).

18. R.G.W. Brown, R. Jones, J.G. Rarity and K.D. Ridley, Characterization of Silicon Avalanche Photodiodes for Photon Correlation Measurements, 2: Active Quenching, Applied Optics, 26, No. 12, 2383-2389 (15 June 1987).

19. RCA Inc., Electro Optics, Silicon Avalanche Photodiodes C30902 and C30921 Series data sheet, (March 1988).

20. A. Lacaida, S. Cova and M. Ghioni, Four-Hundred Picosecond Single-Photon Timing with Commercially Available Avalanche Photodiodes, Rev. Sci. Instrum, 59, No. 7, 1115-1121 (July 1988).

21. A.W. Lightstone and R.J. McIntyre, Photon Counting with Silicon Avalanche Photodiodes for Photon Correlation Spectroscopy, Presented at the O.S.A. Topical Meeting on Photon Correlation Techniques and Applications, May 30-June 2, 1988, Washington, D.C.

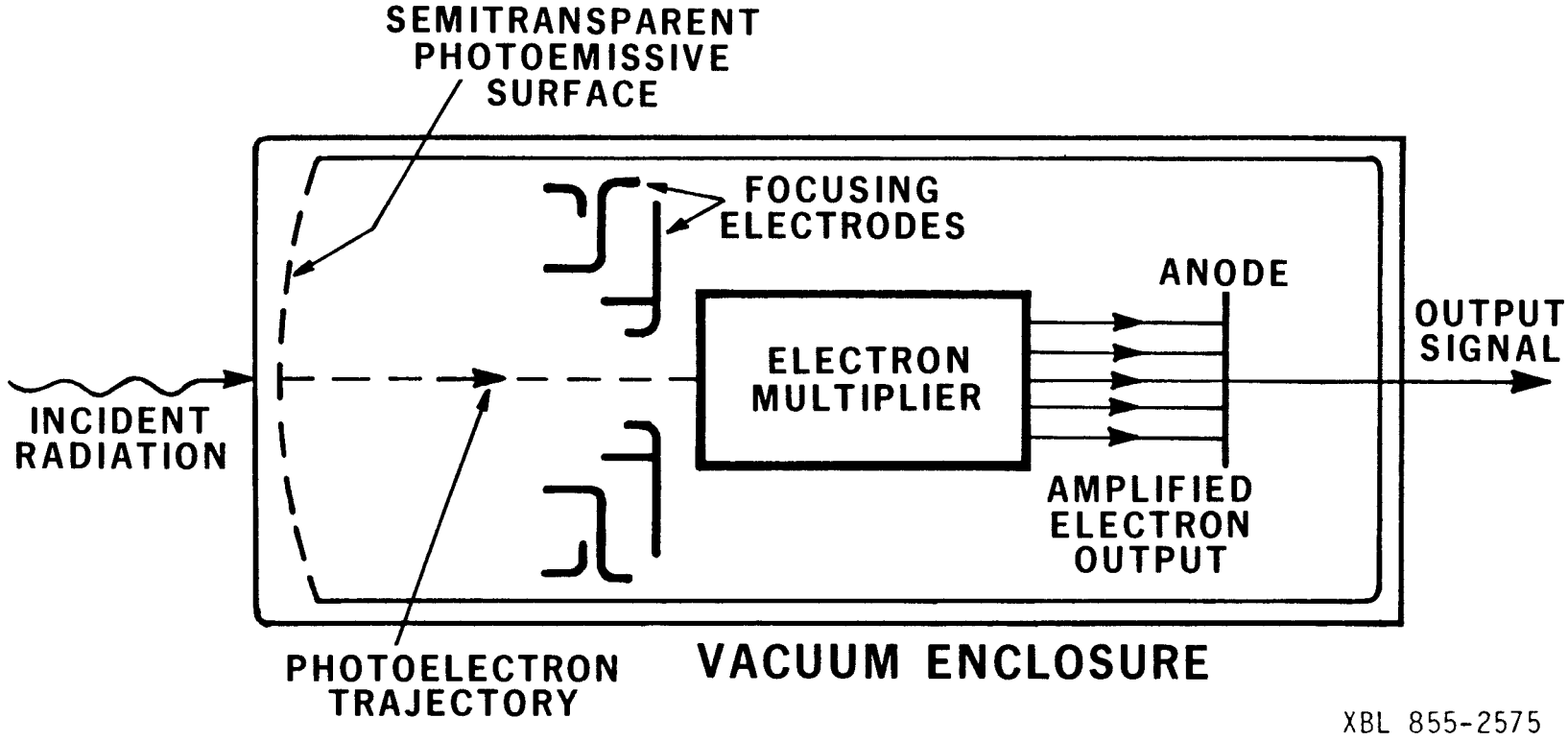

Fig. 1. Simplified component arrangement of a high gain photomultiplier.

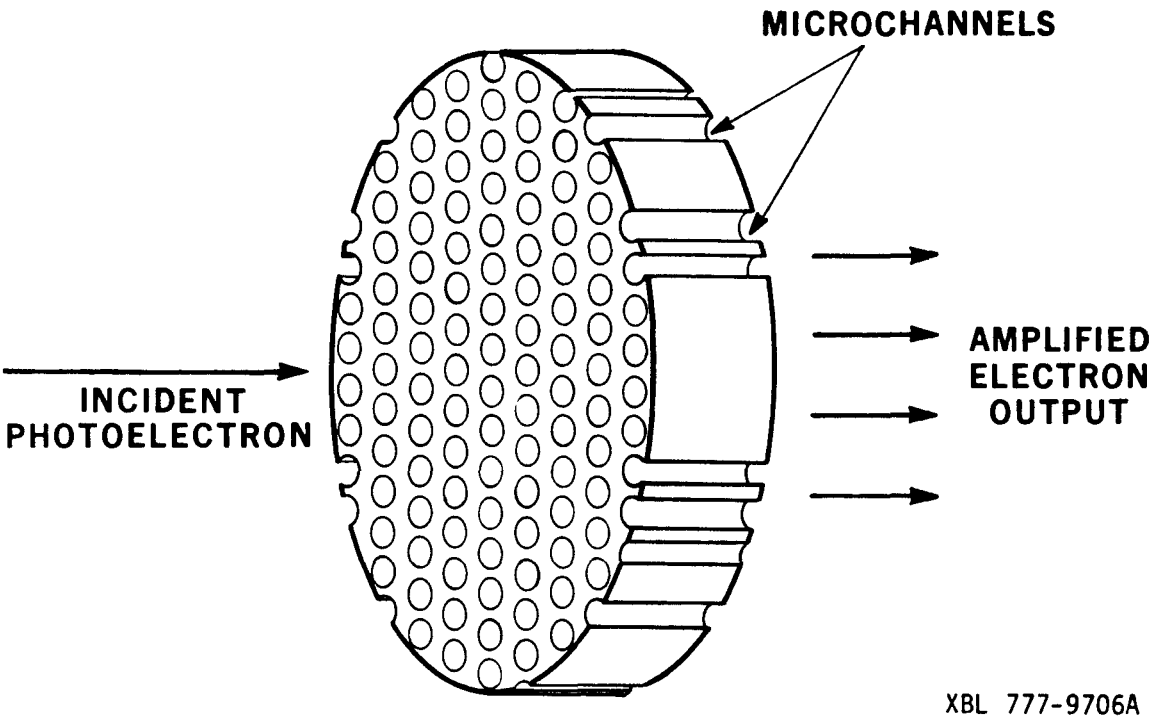

Fig. 2. Microchannel plate electron multiplier.

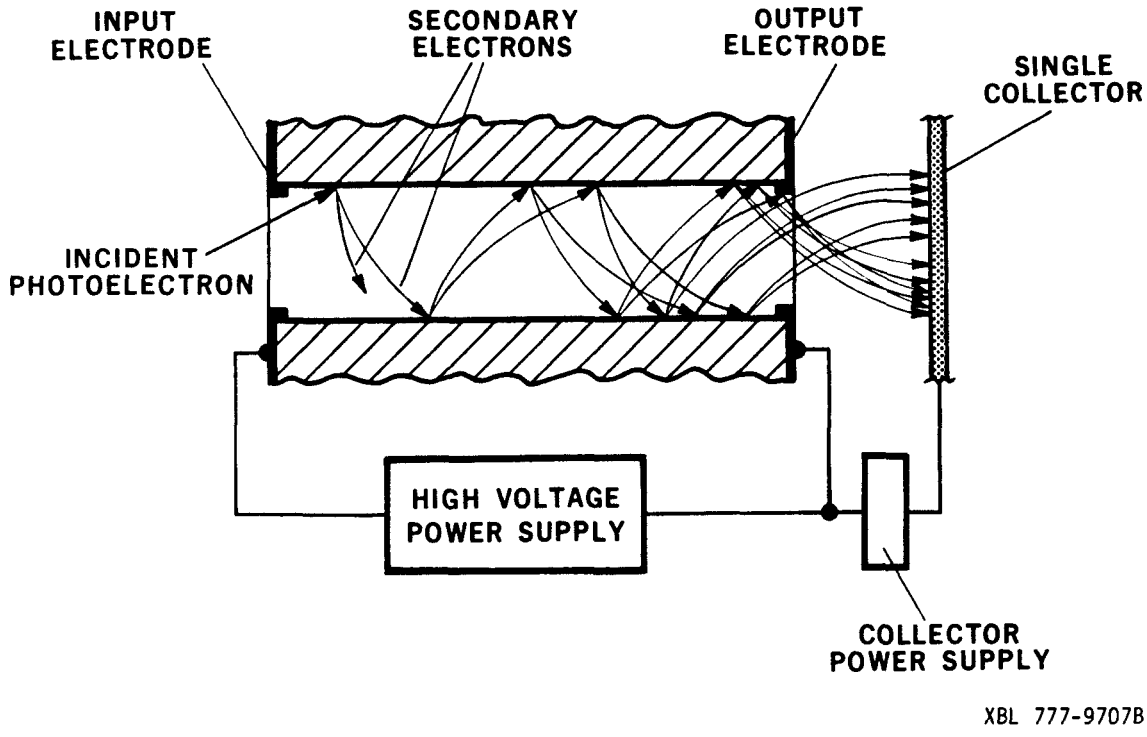

Fig. 3. Multiplication and collection processes in a straight microchannel plate electron multiplier.

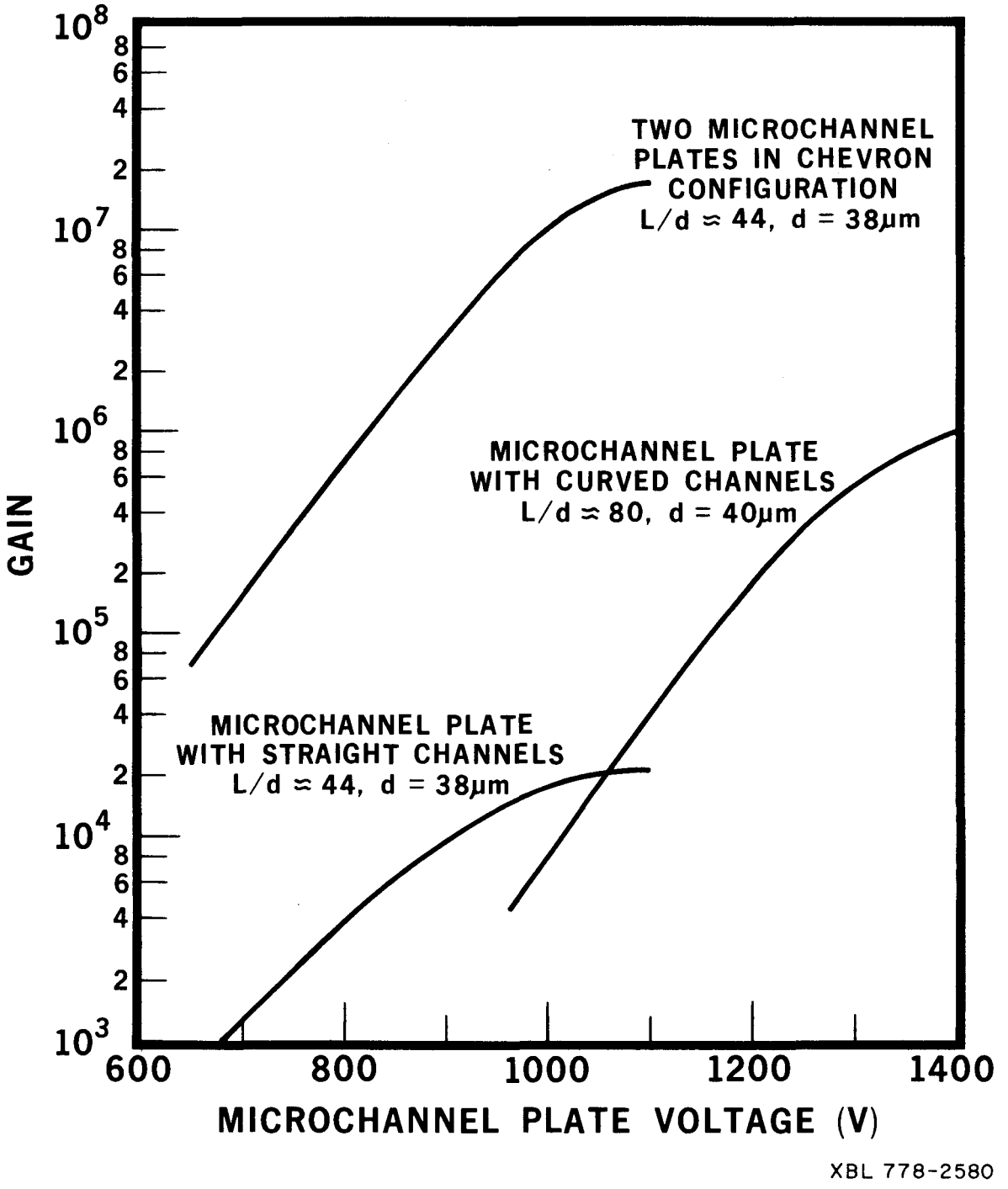

Fig. 4. Microchannel plate gain as a function of the applied voltage per plate.

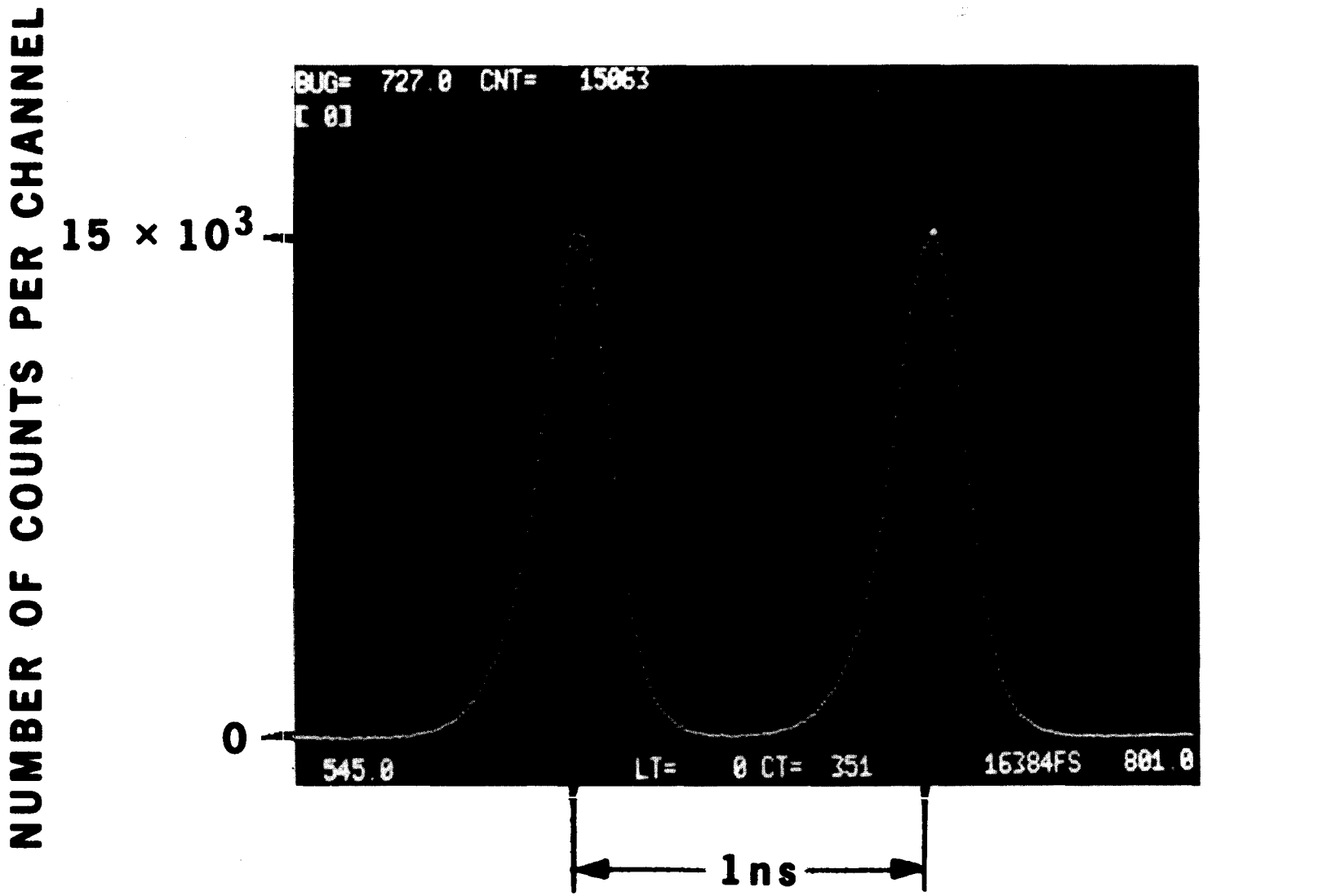

Fig. 5. Single photoelectron time spread of the F4129 photomultiplier with full photocathode illuminated.

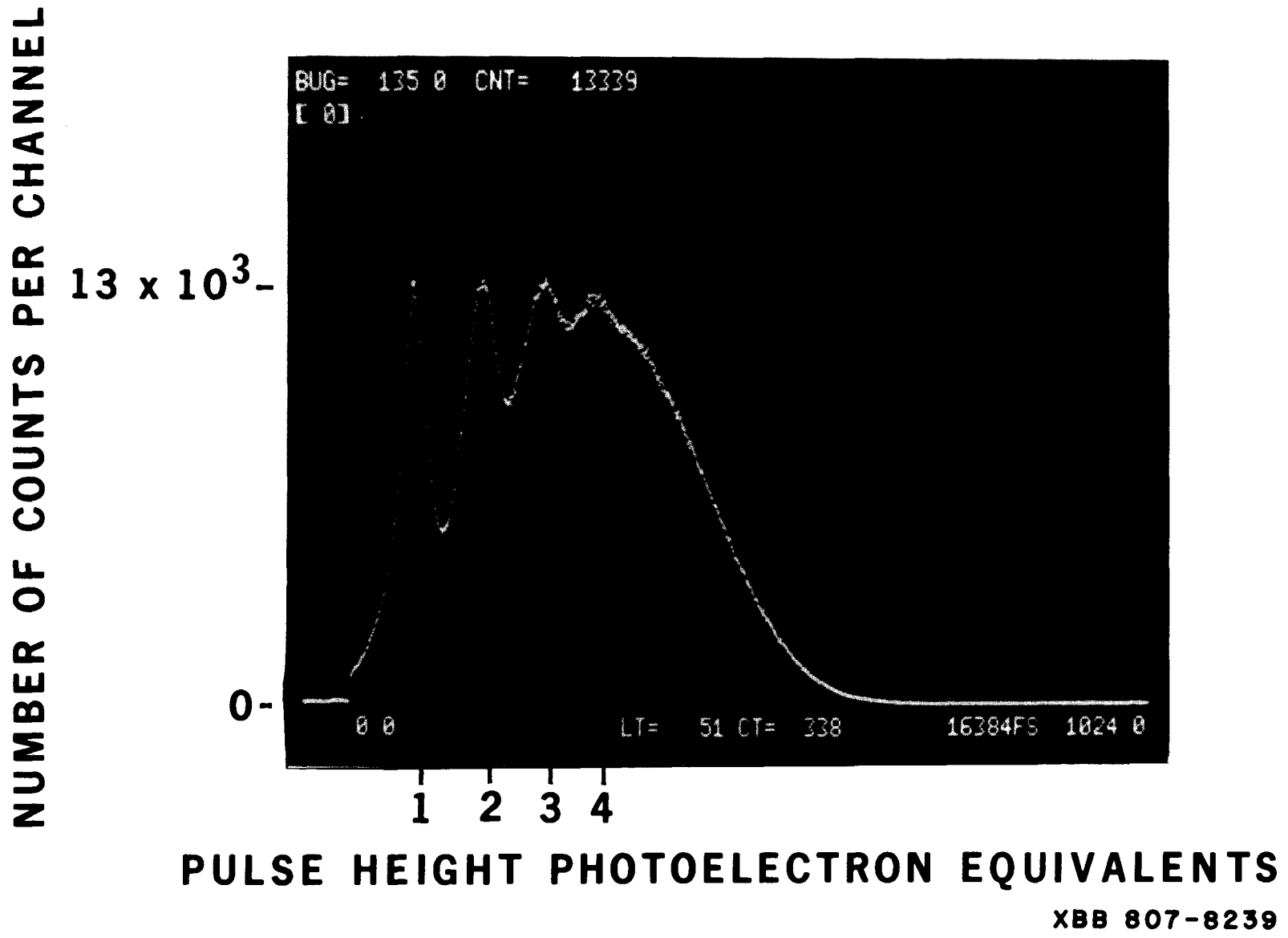

Fig. 6. Pulse-height spectrum of the F4129 operating at microchannel plate cascade voltage of V_M = 2710V.